ISSN 2288-8403(Online)

한국표면공학회지
*J. Surf. Sci. Eng.*
Vol.56, No.4, 2023.
https://doi.org/10.5695/JSSE.2023.56.4.227

〈Research Article〉

# Dielectric relaxation properties in the lead scandium niobate

**Yeon Jung Kim***

College of Engineering, Dankook University, Yongin 448-701, Korea

(Received 11 August, 2023 ; revised 22 August, 2023 ; accepted 23 August, 2023)

**Abstract**

In this study, complex admittance as a function of temperature and frequency was measured to analyze the important relaxation properties of lead scandium niobate, which is physically important, although it is not an environmentally friendly electrical and electronic material, including lead. Lead scandium niobate was synthesized by heat treating the solid oxide, and the conductance, susceptance and capacitance were measured as a function of temperature and frequency from the temperature dependence of the RLC circuit. The relaxation characteristics of lead scandium niobate were found to be affected by contributions such as grain size, grain boundary characteristics, space charge, and dipole arrangement. As the temperature rises, the maximum admittance and susceptance increase in one direction, but the resonance frequency decreases below the transition temperature but increases after the phase transition.

*Keywords : PSN ; Dielectric relaxation ; Cole-Cole diagram ; Thermal fluctuation.*

## 1. Introduction

Unlike $ABO_3$ structures such as $BaTiO_3$ (BT) or $PbTiO_3$ (PT), $A(B',B'')O_3$, $(A',A'')BO_3$ complex perovskites such as $Pb(S_{c1/2}N_{b1/2})O_3$ (PSN), $Pb(M_{g1/3}N_{b2/3})O_3$ (PMN), and $(K_{1/2}Na_{1/2})NbO_3$ (KNN) have a nano-sized crystal structure. It shows relaxation characteristics with strong frequency dependence. When $Sc^{3+}$ and $Nb^{5+}$ ions occupy the center of the body of PSN in a ratio of 1:1, it shows a cubic perovskite structure in the temperature range of about 110℃ or higher. However, diffuse-type ferroelectricity is expressed when the $Sc^{3+}$ and $Nb^{5+}$ ions are in a short range or aligned state [1, 2]. In addition, unlike the properties of PMN or $(Sr,Ba)Nb_2O_6$ (SBN), which are typical diffused ferroelectrics, PSN has aroused great interest in the study of material properties in physics and material engineering due to its short range and unusually interesting properties of nanoscale pole alignment [3]. Since this momentum appears as a thermal fluctuation, it can be clearly observed as a physical parameter reflecting various changes such as dielectric loss, electrical resistance, and heat quantity.

The dielectric loss of PSN, which is relatively large, is not suitable for applications, but the dielectric loss of ferroelectrics causes various characteristic changes in polycrystals with complex microstructures because the movement of charges is converted into lattice, that is, phonon vibration [4, 5]. Although many analyzes have been conducted by physicists and materials scientists, the

*Corresponding Author : Yeon Jung Kim
College of Engineering, Dankook University
Tel: +82-31-8005-3764; E-mai: yjkim80@dankook.ac.kr

specific analysis of the relaxation process of PSN has not been completely analyzed qualitatively and quantitatively.

In order to analyze the frequency-dependent characteristics of the PSN, the complex admittance of the PSN over the temperature range from room temperature to 250 ℃ and the frequency range from 0.1 to 100 kHz with a wide distribution of relaxation phenomena was analyzed by a static method. In addition, the conductance and susceptance of the PSN were analyzed together to find out the widely broad distributed relaxation phenomenon.

## 2. Experiment Procedure

In this study, the process of synthesizing B-site Wolframite $ScNbO_4$ powder with $PbCO_3$, which is widely used in the production of perovskite-structured PSN, was not applied. Instead, PSN specimens were first mixed with starting oxides such as $PbCO_3$, $Sc_2O_3$ and $Nb_2O_5$, calcined at 900 ℃ and sintered at 1400 ℃, and the holding times of the two heat treatment steps were 2 h and 20 min, respectively [6]. The phase and crystallinity of the specimens were investigated by XRD, with an XRD scan rate of 2 °/min and a step size of 0.02°. In addition, the atomic composition of the compound was analyzed by EDX, and the surface of the specimen was observed using SEM. To measure the physical quantities, a PSN thick film was polished to a thickness of 1 mm, and a 99.9% high-purity silver electrode was deposited with a diameter of 2 cm and 1.8 cm on both sides using a thermal evaporator, respectively, to manufacture the electrode and suppress the edge effect as much as possible. Resistance, inductance and capacitance were measured as a function of temperature and frequency of the samples coated with silver electrodes using an HP 4284A LCR meter.

## 3. Results and Discussion

Figure 1 shows the XRD pattern of the PSN specimen. The perovskite phase was well formed in the sample sintered at 1400 ℃, which is slightly higher than in the previous experiment. The inset in Figure 1 is a SEM image of the PSN specimen. Chemically synthesized oxides PSN are known to be in a completely B-site disordered form. As shown in the Figure 1, since it was synthesized under appropriate sintering conditions, the crystal grains of the fractured surface of the sample increased, while the pores decreased. Similar to the trend reported previously, the atomic occupancy of $Pb^{2+}$, $Sc^{3+}$, $Nb^{5+}$ and $O^{2-}$ ions in the sintered body was confirmed to be 17.01~17.02%, 8.95~8.96%, 10.57~10.59% and 63.42~63.47%, respectively.

Dielectric relaxation is closely related to the role of dipoles in molecules, ions and electrons. The frequency dependence of ferroelectric properties is simply expressed as Y*=G+jB. In this complex function, Y* is admittance, G is conductance, and B is susceptance. Also, the complex dielectric constant associated with dielectric dispersion is given by $\varepsilon^*(\omega)=\varepsilon'(\omega)-j\varepsilon''(\omega)$, where $\varepsilon'(\omega)$ is the real dielectric constant and $\varepsilon''(\omega)$ is the imaginary dielectric constant. In this relationship, $G(\omega)$, $\varepsilon'(\omega)$ and $\varepsilon''(\omega)$ are closely related to the dipole alignment by the electric field and the energy loss rate during dipole rotation. Therefore, it is reasonable

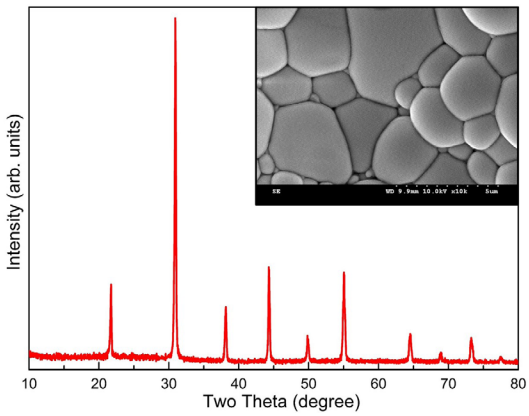


Fig. 1. Typical XRD patterns of the PSN specimen sintered at 1400 ℃ for 2h. The inset in Figure 1 is a SEM image of the PSN specimen.

to reported that dielectric relaxation, which determines physical properties, is directly related to defect concentration [7].

The complex admittance and complex dielectric constant can be expressed by the two equations $Y^*(\omega) = \frac{1}{Z^*(\omega)} = G + jB = j\omega C_o \varepsilon^*$ and $\frac{\varepsilon^*(\omega)}{\varepsilon_s - \varepsilon_\infty} = \frac{1}{1+(j\omega\tau)^{1-\alpha}}$, where $Z(\omega)^*$ is the complex impedance. In the two equations, the angular frequency is $\omega = 2\pi f$, the geometric capacitance is $C_o = \varepsilon_o A/d$, the permittivity of free space is $\varepsilon_o (=8.854\times10^{-12}$ F/m), the area of the electrode is A, and the spacing of the electrodes is d. In addition, $\varepsilon_\infty$ and $\varepsilon_s$ are the high- and low-frequency values of the dielectric constant, respectively, and $\alpha$ is the relaxation time distribution $\tau = \tau_o e^{E_a/k_B T}$. In the relaxation time equation, $\tau_o$ is the pre-exponential factor, $E_a$ is the activation energy, and $k_B$ is the Boltzmann constant.

Figure 2 is a plot of resistance and inductance as a function of temperature for PSN sintered at 1400 ℃ for 20 minutes. The RLC series circuit inserted in Figure 2 is a circuit diagram of resistance and inductance. Resistance and inductance measured at 20~150 ℃ were calculated as 16.8~2.55 Ω and $4.74\times10^{-6}$~$5.20\times10^{-6}$ H, respectively. And the calculated series capacitance value increased from $1.48\times10^{-10}$ F to $2.98\times10^{-9}$ F with increasing temperature, and the parallel capacitance slightly increased from $1.55\times10^{-20}$ F to $3.87\times10^{-19}$ F with increasing temperature.

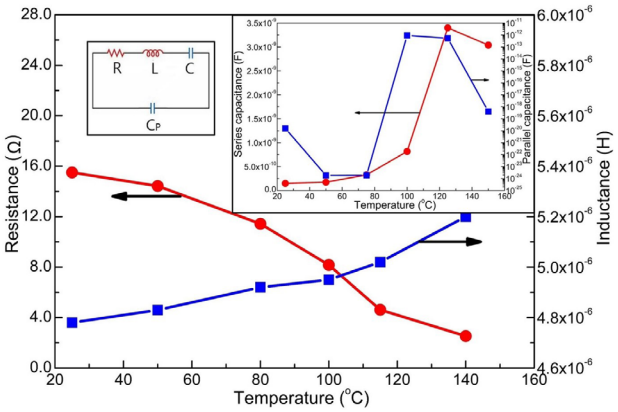


Fig. 2. Plot of resistance and inductance as a function of temperature for PSN sintered at 1400 ℃ for 20 minutes. The RLC series circuit inserted in Figure 2 is a circuit diagram of resistance and inductance.

Figure 3 shows the frequency dependence of inductance and susceptance of the PSN measured in the temperature range of 20 to 150 ℃. As shown in the figure, the change in frequency of inductance and susceptance was very distinct. As shown in Figure 3, the characteristics of inductance and susceptance of lead-type perovskite were shown, and the two peak values increased as they moved from room temperature to the phase transition temperature. Like the strong temperature dependence of the resistance and inductance of the PSN, the capacitance is also sensitive to temperature and the resonant frequency changes with it. Therefore, as the measurement temperature increases, inductance and susceptance broaden in the high frequency band, and as a result, the phenomenon of relaxation process and diffusion phase transition is observed. This change in symmetry is associated with a change in polarization direction as well as a change in polarization magnitude and extinction of relaxation [8]. In general, since the dielectric properties of a ferroelectric according to temperature and frequency can be obtained by analyzing a Cole-Cole diagram, an important dielectric relaxation phenomenon can be understood in PSN [9].

Figure 4 is a Cole-Cole diagram to analyze the contribution due to the microscopic amount of PSN using the data in Figure 3. When the conductance vs. susceptance relationship is

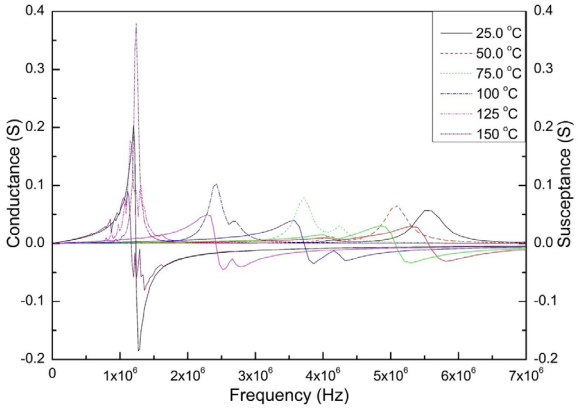


Fig. 3. Frequency dependence of conductance and susceptance of measured in the temperature range of 25 to 150 ℃.

analyzed as a function of frequency according to the six measured temperatures, the conductance characteristics are analyzed to be due to the release of space charges as the frequency increases, as shown in Figure 3. In addition, as shown in Figure 4, the large change in conductance versus susceptance was further magnified as the temperature increased, which is analyzed as a dielectric relaxation characteristic of PSN in a form different from that of the Debye type.

Figure 5 is the data obtained by measuring the dielectric constant and dielectric loss under the condition of a temperature rise and fall rate of 4 ℃/min. Also, Figure 5 shows the abnormal relaxation time distribution that differs from the normal relaxation time characteristics of PSN ferroelectrics. The relaxation properties of most ferroelectrics are related to the reduction of short- and long-time polarization. Of course, the long-time relaxation is further diffused by the activation of electrical conduction as the temperature increases, which is sensitive to the complex admittance and complex dielectric constant of $Sc^{3+}$ and $Nb^{5+}$ ions occupying the body center of PSN in a 1:1 ratio. The relaxation characteristics of PSN and, in particular, the shift of the $Pb^{2+}$ position of the cube-corner site as the existence of a partial polar domain on the high-temperature side even if it has a cubic structure after the phase transition is completed. Figure 5 clearly shows the thermal fluctuation during heating and cooling measurements of the PSN specimen. These abnormal characteristics can be analyzed as freezing of the nanoclusters occurs at a temperature lower than the phase transition temperature (~119 ℃ for heating process, ~107 ℃ for cooling process) of PSN, when measured while decreasing the temperature. It can be said that these thermal fluctuations show the diffusion phase transition characteristics of the disordered PSN specimen. This is a characteristic that the PSN specimen shows several transition points, just as complex perovskites such as PMN and SBN have multiple transition points. PSN specimens have a rhombohedral crystal structure below the transition temperature. Also, the maximum values of the dielectric constant and dielectric loss of the PSN specimen were measured at ~36700 and ~0.020 during the heating process and ~37500 and ~0.022 during the cooling process, respectively. In addition, in Figure 5, the transition temperature during the heating and cooling processes was ~119 ℃ and ~107 ℃, respectively, with a change of about 12 ℃. And the maximum value of the dielectric loss under the same experimental conditions was ~112 ℃ and ~92 ℃, respectively, showing a large difference of about 20 ℃. As shown in Figure 5, the difference between the transition temperature and the maximum dielectric loss temperature in the heating process was about 7 ℃, and about 15 ℃ was measured in the cooling process. This phenomenon

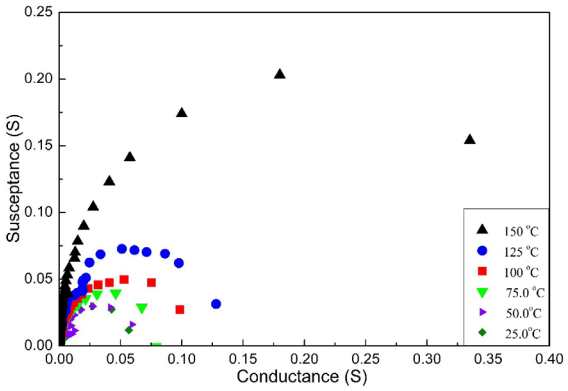


Fig. 4. Cole-Cole diagram for susceptance vs. conductance of PSN as a function of temperature to analyze the contribution due to the microscopic amount of PSN using the data in Figure 3.

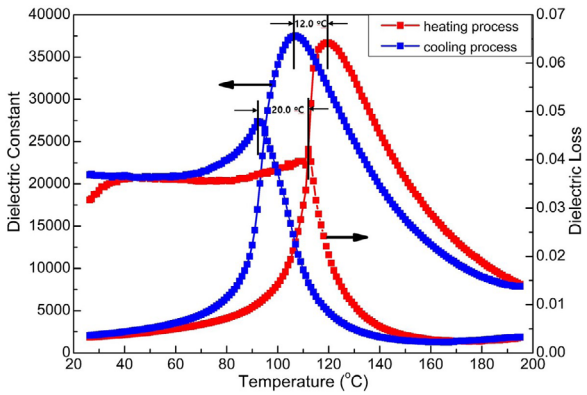


Fig. 5. Plot of temperature dependence of dielectric constant and dielectric loss under the condition of a temperature rise and fall rate of 4 ℃/min at 1 kHz.

is considered to be that as more energy is required for dipole rotation as the transition temperature approaches, the dielectric loss increases rapidly. Considering that a large dielectric dispersion was observed near the phase transition as shown in Figure 5, the measured dielectric constant can be said to be typical of a typical diffuse ferroelectric [7]. This is because even after the completion of the phase transition, the thermal energy is sufficient to equalize the six equilibrium positions in the unit cell of the PSN, so the total electric dipole moment of the PSN specimen still remains. Most dipoles of dielectrics are statistically ordered by electric field or thermal energy below the transition temperature, but become random and disordered at higher temperatures. Of course, the dielectric response of a diffused ferroelectric is a combination of domain/ domain wall movement and lattice defects. This behavior is similar to the freezing of nanoclusters that occurs around room temperature. The dielectric properties of dense dielectrics are measured very stably, but the dielectric dispersion widens near the phase transition. Due to the transition from the unpolarized state to the polarized state, the dielectric constant exhibited typical diffuse ferroelectric properties. These phenomena are known as the most common characteristics of the diffusion phase transition due to composition fluctuations and microscopic non-inhomogeneity. In the 21st century, research on lead-type diffused ferroelectrics has been stagnant due to the increased demand for eco-friendly materials, but the transition to eco-friendly materials has not yet entered in earnest. Currently, research on the dielectric relaxation of lead-free diffused ferroelectrics is mainly focused, but it is eventually based on research on the properties of lead-type ferroelectrics as prototypes [10~15]. Also, when measured while increasing the temperature, the resistance of the PSN decreases continuously as shown in Figure 2, that is, it is in good agreement with the phenomenon of negative temperature coefficient of resistance (NTCR).

## 4. Conclusions

Although the traditional oxide mixing method was used, $PbCO_3$, $Sc_2O_3$, and $Nb_2O_5$ were reacted in one-step without the primary synthesis of wolframite, a method widely applied in the manufacture of complex perovskite, to prepared an ideal perovskite PSN without the appearance of a pyrochlore phase. The maximum conductance and inductance of the complex admittance and dielectric constant of the perovskite PSN as a function of temperature and frequency increased as the measured temperature increased. The complex admittance data of PSN agree well with the relaxation characteristics, and the capacitance increased at the transition but decreased slowly thereafter. In addition, when the temperature of the PSN specimen was continuously raised, the resistance decreased inversely proportionally, but the inductance increased proportionally, showing an abnormal ferroelectric characteristic.

## References

[1] J. W. Hyun, J. D. Byun, Y. J. Kim, G. B. Kim, K. A. Lee, Ferroelectric and Dielectric Properties of the $Pb(Sc_{1/2}Nb_{1/2})O_3$ Ceramic System, Journal of the Korean Physical Society, 57 (2010) 485-488.

[2] J. L. Tang, M. K. Zhu, Y. D. Hou, H. Wang, H. Yan, Effect of pH value on phase structure, component, and grain morphology of $Pb(Sc_{1/2}Nb_{1/2})O_3$ powders by precipitation method, Journal of Crystal Growth, 307 (2007) 70-75.

[3] F. Chu, I. M. Reaney, N. Setter, Spontaneous (zero-field) relaxor to ferroelectric phase

ransition in disordered $Pb(Sc_{1/2}Nb_{1/2})O_3$, Journal of Applied Physics, 77 (1995) 1671-1676.

[4] A. A. Bokov, Z. G. Ye, Dielectric relaxation in relaxor ferroelectrics, Journal of Advanced Dielectrics, 2 (2012) 1-24.

[5] C. Zhao, C. Z. Zhao, M. Werner, S. Taylor, P. Chalker, Dielectric relaxation of high-k oxides, Nanoscale Research Letters, 8 (2013) 456-474.

[6] J. W. Hyun, J. D. Byun, Y. J. Kim, Raman and dielectric spectroscopy in the disordered $Pb(Sc_{1/2}Nb_{1/2})O_3$ relaxor fabricated by one-step mixed oxide method, Journal of the Korean Physical Society, 66 (2015) 1057-1061.

[7] A. Chen, J. F. Scott, Y. Zhi, H. Ledbetter, J. L. Baptista, Dielectric and ultrasonic anomalies at 22K, 37K and 65K in $SrTiO_3$, Physical Review B, 59 (1999) 6661-6668.

[8] J. M. Kiat, C. Bogicevic, F. Karolak, G. Dezanneau, N. Guiblin, W. Ren, L. Bellaiche, R. Haumont, Low-symmetry phases and loss of relaxation in nanosized lead scandium niobate, Physical Review B, 81 (2010) 144122.

[9] R. Padhee, P. R. Das, B. N. Parida, R. N. P. Choudhary, Impedance analysis of $K_2Pb_2X_2W_2Ti_4Nb_2O_{30}$ (X=Nd, Y) tungsten bronze ceramics, Journal of the Korean Physical Society, 64 (2014) 1022-1030.

[10] X. Li, X. Fan, Z. Xi, P. Liu, W. Long, P. Fang, F. Guo, R. Nan, Dielectric relaxor and conductivity mechanism in Fe-substituted PMN-32PT ferroelectric crystal, Crystals, 9(5) (2019) 241-247.

[11] R. Das, R.N.P. Choudhary, Solid State Sciences, Studies of structural, dielectric relaxor and electrical characteristics of lead-free double Perovskite:$Gd_2NiMnO_6$, Solid State Sciences, 87 (2019) 1-8.

[12] Z. Raddaoui, S. E. Kossi, J. Dhahri, N. Abdelmoula, K. Taibi, Study of diffuse phase transition and relaxor ferroelectric behavior of $Ba_{0.97}Bi_{0.02}Ti_{0.9}Zr_{0.05}Nb_{0.04}O_3$ ceramic, RSC Advances, 9 (2019) 2412-2425.

[13] W. Dong, B.X. Wang, Y. Yuan, H. Wu, A. A. Bokov, Z.G. Ye, Synthesis, structural evolution, and dielectric properties of a new perovskite solid solution $(Pb_{0.5}Sr_{0.5})(Zr_{0.5}Ti_{0.5})O_3$-$PbTiO_3$, Journal of the American Ceramic Society, 105 (2022) 4775-4783.

[14] C. J. Chang, X. Qi, Dielectric relaxation and high recoverable energy density in $(1-x)(0.3BiFeO_3-0.7SrTiO_3)-xK_{0.5}Na_{0.5}NbO_3$ ceramics, Ceramics International, 48 (2022) 25610-25620.

[15] S. Singh, A. Kaur, P. Kaur and L. Singh, High-temperature dielectric relaxation and electric conduction mechanisms in a $LaCoO_3$-modified $Na_{0.5}Bi_{0.5}TiO_3$ system, ACS Omega, 8 (2023) 25623-25638.